NUMERICAL MODELLING OF HEAT TRANSFER AND HYDRODYNAMICS IN LASER-PLASMA TREATMENT OF METALLIC MATERIALS*

Yu.S. BORISOV, V.F. DEMCHENKO, A.B. LESNOJ, V.Yu. KHASKIN and **I.V. SHUBA**
E.O. Paton Electric Welding Institute, NASU
11 Bozhenko Str., 03680, Kiev, Ukraine. E-mail: office@paton.kiev.ua

An approximate mathematical model is proposed to describe thermal and hydrodynamic processes occurring in combined laser-plasma cladding. The scheme of a rapidly moving heat source, which generalises the known N.N. Rykalin's scheme for a case of combined convective-conductive heat transfer in molten metal, is considered. Densities of the different-power laser and plasma heat sources are assumed to be distributed on the plate surface by the normal law, having different radii of heat spots. The combined heat spot is assumed to be additive. The equation of local heat balance on the surface of a workpiece allows for heat transfer by radiation and heat losses for evaporation. It is assumed that motion of the melt under the indirect-action plasma heating conditions is driven by the Archimedes buoyancy force and thermocapillary force. Verification of the mathematical model was carried out, and results of calculation experiments on investigation of the penetration zone under the effect of the laser and combined laser-plasma heat sources are described. It is shown that the Marangoni force is a dominant force factor determining hydrodynamics of the melt. The effect of convective energy transfer on formation of the molten zone was studied. 8 Ref., 4 Tables, 8 Figures.

Keywords: *laser-plasma cladding, thermal and hydrodynamic processes, modelling, heat transfer, heat balance, cladding, penetration zone, Marangoni force*

Problem statement. One of the topical problems of welding, cladding and other metal treatment technologies using plasma-arc, laser or combined laser-plasma heating is evaluation of results of the thermal impact by the heat source on a workpiece. There are many publications dedicated to the issues of theoretical and experimental investigation of the laser and plasma-arc effect on metallic materials [1–3]. At the same time, the problem of the combined effect on metals by the microplasma arc (of a direct or indirect action) and laser beam, the interest in which has dramatically grown with emergence of the combined laser-microplasma technologies, is studied to a much lower degree.

For adequate theoretical description of the processes occurring in laser-microplasma cladding of metallic materials it is necessary to take into account the complex interaction of different physical processes and phenomena related to heating and melting of the base material under the effect of the combined heat source. It can be assumed with a sufficiently good approximation that the combined laser-microplasma energy source is additive, i.e. it can be represented as a sum of the laser and microplasma heat sources distributed on the workpiece surface.

Normally, the models of the heat source generated by laser radiation allow for absorption of the laser radiation by a metallic material and set some law of distribution of the power density on the surface of a material treated. It should be noted in analyses of a plasma component of the heat flow that combined laser-microplasma cladding is performed as a rule by using the indirect-action plasmatrons, i.e. the current does not flow through the workpiece.

Nevertheless, thermal interaction of the current-free plasma with the workpiece surface occurs due to transfer of the critical and potential energy of the plasma particles, this resulting in the formation of the law of distribution of the plasma the heat source thermal power.

Under the thermal effect of the heat source with a density of 10^4 W/cm^2 and higher, the temperature of the weld pool surface may be 10–20 K higher than the boiling temperature, as a result of which the heat losses for evaporation do not only exceed the heat losses due to convective and radiant heat exchanges taken together, but also become comparable with the den-

*The article is based on the presentation made at the 6th International Conference «Mathematical Modelling and Information Technologies in Welding and Related Processes» (29 May–1 June, 2012, Katsiveli, Ukraine).

sity of the heat source. Therefore, allowance for the evaporation heat is an important aspect of theoretical description of the thermal effect by the combined laser-plasma heat source on the material treated.

Mathematical model. Proceed from an assumption that formation of the molten metal zone takes place in a heat conduction mode. This term implies a mode in which the penetration zone of the base metal forms without formation of a pronounced keyhole.

According to this, the free surface of the molten metal is assumed to be non-deformed, and the heat source affecting the workpiece is assumed to be the surface one.

Despite a small volume of the melt forming in cladding by using the combined laser-microplasma energy source, the velocity of motion of the liquid metal in the molten metal may be sufficiently high. Hence, the convective energy transfer can play a marked role in formation of the thermal state of the workpiece being treated.

At the absence of the current flowing through the metal pool, the Archimedes thermal buoyancy force and Marangoni thermocapillary force are the force factors affecting the molten metal.

Let $\{x', y', z'\}$ be the fixed system of Cartesian coordinates related to the workpiece being welded, the z' axis of which is directed along the gravity line; and t' be the time. Add the $\{x, y, z\}$ moving coordinate system as follows: $x = x' - v_w t'$, $y = y'$, $z = z'$, and $t = t'$, where v_w is the speed of movement of the heat source.

Upon reaching the quasi-stationary thermal and hydrodynamic state, the complete system of the hydrodynamics and heat exchange equations can be written down as follows:

$$(V_x + v_w)\frac{\partial W}{\partial x} + V_y\frac{\partial W}{\partial y} + V_z\frac{\partial W}{\partial z} = \quad (1)$$
$$= \frac{\partial}{\partial x}\left(\lambda\frac{\partial T}{\partial x}\right) + \frac{\partial}{\partial y}\left(\lambda\frac{\partial T}{\partial y}\right) + \frac{\partial}{\partial z}\left(\lambda\frac{\partial T}{\partial z}\right);$$

$$\begin{cases} (V_x + v_w)\dfrac{\partial V_x}{\partial x} + V_y\dfrac{\partial V_x}{\partial y} + V_z\dfrac{\partial V_x}{\partial z} = -\dfrac{1}{\rho}\dfrac{\partial P}{\partial x} + \nu\Delta V_x; \\ (V_x + v_w)\dfrac{\partial V_y}{\partial x} + V_y\dfrac{\partial V_y}{\partial y} + V_z\dfrac{\partial V_y}{\partial z} = -\dfrac{1}{\rho}\dfrac{\partial P}{\partial y} + \nu\Delta V_y; \\ (V_x + v_w)\dfrac{\partial V_z}{\partial x} + V_y\dfrac{\partial V_z}{\partial y} + \\ + V_z\dfrac{\partial V_z}{\partial z} = -\dfrac{1}{\rho}\dfrac{\partial P}{\partial z} + \nu\Delta V_z + g\beta_T T; \\ \dfrac{\partial V_x}{\partial x} + \dfrac{\partial V_y}{\partial y} + \dfrac{\partial V_z}{\partial z} = 0, \end{cases} \quad (2)$$

where V_x, V_y and V_z are the components of the melt velocity vector; ν is the kinematic viscosity; P is the pressure; β_T is the thermal coefficient of volume expansion of the melt; g is the gravity acceleration; $W = \rho\int_0^T c\,dT + \rho\chi\eta$ is the enthalpy; ρ is the density; c is the specific heat of the material; T is the temperature; χ is the latent solidification heat; λ is the thermal conductivity factor; $\eta = (T, T_S, T_L)$ is the volume fraction of the liquid phase in the solidification temperature range; and T_S and T_L are the solidus and liquidus temperatures. Equation (1) is integrated in the $\Omega = \Omega_L \cup \Omega_S$ region, where Ω_L is the weld pool, and Ω_S is the non-melted base metal. Equation system (2) is determined in the Ω_L region.

Let $\mathrm{Pe} = (v_w l)/a$ be the Peclet thermal criterion, where l is the characteristic geometrical dimension (in this case, it is the thickness of the plate treated), and a is the thermal conductivity coefficient of the deposited material. At $\mathrm{Pe} >> >> 1$, the rapidly moving source scheme suggested by N.N. Rykalin [4] for the welding heat model formulated within the frames of the conductive mechanism of heat transfer in a workpiece is a good approximation of the three-dimensional problem for calculation of the temperature field. In the present study, the idea of the rapidly moving source covers a case of the combined convective-conductive energy transfer. The rapidly moving source scheme ignores the heat transfer in a direction of the welding heat source, the allowance being made only for the heat transfer across the workpiece treated. In addition to the above-said, assume in equations (2) that $V_x = 0$ and $\partial P/\partial x = 0$. Then the systems of equations (1) and (2) can be written down in the following form:

$$\frac{\partial W}{\partial \tau} + V_y\frac{\partial W}{\partial y} + V_z\frac{\partial W}{\partial z} = \quad (3)$$
$$= \frac{\partial}{\partial y}\left(\lambda\frac{\partial T}{\partial y}\right) + \frac{\partial}{\partial z}\left(\lambda\frac{\partial T}{\partial z}\right), \quad y, z \in \Omega^*;$$

$$\begin{cases} \dfrac{\partial V_y}{\partial \tau} + V_y\dfrac{\partial V_y}{\partial y} + V_z\dfrac{\partial V_y}{\partial z} = -\dfrac{1}{\rho}\dfrac{\partial P}{\partial y} + \nu\Delta V_y; \\ \dfrac{\partial V_z}{\partial \tau} + V_y\dfrac{\partial V_z}{\partial y} + V_z\dfrac{\partial V_z}{\partial z} = -\dfrac{1}{\rho}\dfrac{\partial P}{\partial z} + \nu\Delta V_z + g\beta_T T; \\ \dfrac{\partial V_y}{\partial y} + \dfrac{\partial V_z}{\partial z} = 0; \\ y, z \in \Omega_L^*, \end{cases} \quad (4)$$

where $\tau = x/v_w$, and $\Omega^* = \{0 < y < L_y,\ 0 < z < L_z\}$ is the cross section of the plate. Hydrodynamics equations (4) are integrated in the Ω^*_L region to be determined, which is limited by the free surface of the melt and solidification front. Geometry of the region is subject to determination from solution of the thermal problem.

Write down the boundary conditions for equation (3) in the following form:

$$\lambda \left.\frac{\partial T}{\partial z}\right|_{z = L_z} = \alpha[T(y, L_z, t) - T_{amb}] + \varepsilon\sigma[\overline{T}^4(y, L_z, t) - \overline{T}^4_{amb}]; \quad (5)$$

$$-\lambda \left.\frac{\partial T}{\partial z}\right|_{z = 0} = \alpha[T(y, 0, t) - T_{amb}] + \varepsilon\sigma[\overline{T}^4(y, 0, t) - \overline{T}^4_{amb}] + q_v(T) + q_h(y, t); \quad (6)$$

$$\left.\frac{\partial T}{\partial y}\right|_{y = 0} = 0, \quad \left.\frac{\partial T}{\partial y}\right|_{y = L_y} = 0, \quad (7)$$

where α is the heat transfer coefficient; T_{amb} is the ambient temperature; ε is the reduced emissivity of the surface; σ is the Stefan–Bolzmann constant; $\overline{T}$ is the absolute temperature; $q_v(T)$ are the heat losses for evaporation; and q_h is the density of the heat flow imparted to the workpiece surface by the plasma and laser heat sources. The heat losses for evaporation from the melt surface were evaluated by using the Knight model [5, 6].

Set distributions of heat flow density $q_h(y, t)$ both for the laser radiation and plasma energy sources in the following form:

$$q_h(y, t) = q_0 \exp(-k(\sqrt{(x_0 - v_w t)^2 + y^2})^n),$$

where x_0 is the initial displacement of the source centre from the origin of fixed coordinate system $\{x', y', z'\}$. Designate the efficient radii of the laser and plasma energy sources through r_L and r_P (it is assumed that 95 % of power of a corresponding source is released at the spot of the efficient radius), $a = \max\{r_L, r_P\}$. If x_0 is assumed to be equal to $x_0 = 1.2a$, at the origin of the moving coordinate system at $t = 0$ the density of the heat flow from the combined laser-plasma heat sources will practically be equal to zero.

Assuming the free surface of the melt to be non-deformed, write down the boundary conditions for hydrodynamics equations (4) in the following form:

$$V_z|_{z = 0} = 0, \quad v \left.\frac{\partial V_y}{\partial z}\right|_{z = 0} = -\frac{\beta_\sigma}{\rho} \left.\frac{\partial T}{\partial y}\right|_{z = 0}, \quad (8)$$

where $\beta_\sigma = \dfrac{d\sigma}{dT}$, and $\sigma = \sigma(T)$ is the coefficient of surface tension of the melt. The second of these conditions is a balance of tangential stresses written down allowing for the effect of the Marangoni thermocapillary force. The adhesion and impermeability conditions are assumed to take place at the solidification front, the following symmetry conditions being set at $y = 0$:

$$V_y|_{y = 0} = 0, \quad \left.\frac{\partial V_z}{\partial y}\right|_{y = 0} = 0. \quad (9)$$

Numeric implementation of the formulated model was carried out by using the Lagrangian–Eulerian method and schemes of splitting of equations (3) and (4) into physical sub-processes and spatial variables [7, 8].

Calculation results. The model was verified by conducting experimental studies of the shape of the penetration and heat-affected zones under the effect on the 09G2S steel plate with thickness $L_z = 1$ cm by the Nd:YAG laser source with power $P_L = 1.25$ kW (focusing lens diameter $D_F = 5$ cm, focusing lens beam diameter $D_L = 4$ cm, lens focal distance $F = 30$ cm, heat source speed $v_w = 60$ m/h). In numerical investigations, the effect of the hydrodynamic factor on formation of the molten zone of the base metal was analysed in the following variants:

- by ignoring convection of the melt;
- by allowing only for free convection;
- by allowing for the thermocapillary force effect;
- by allowing for the combined effect of the thermal buoyancy and thermocapillary forces.

Table 1. Effect of hydrodynamic factors on penetration parameters

No.	Type of evaluation		H, cm	B, cm	V_y, cm/s	V_z, cm/s	T_{max}, °C
	Experiment		0.042	0.222	–	–	–
1	Calculation	Without convection	0.051	0.168	0	0	2905
2		A	0.049	0.174	0.191	0.089	2896
3		M	0.045	0.234	51.101	16.205	2875
4		A + M	0.042	0.252	51.300	16.310	2874

Note. A — free convection; M — Marangoni convection.

The calculation results obtained at $\eta = 0.32$ and $r_L = 0.1$ cm are given in Table 1 and shown in Figure 1. The Table gives the calculation data on penetration width B and depth H, as well as on the value of maximal overheating of the metal pool surface and maximal values of components of the melt velocity vector. It follows from Table 1 that the closest coincidence of the calculation and experimental data is achieved at the effect on the melt by the thermal buoyancy and thermocapillary forces, the dominant factor determining the penetration width being the Marangoni thermocapillary convection.

Direction of the flow of the melt and its velocity (~50 cm/s) are governed by the dominant action of the Marangoni force, under the effect of which the flows of the melt transfer the most overheated metal from the paraxial part of subsurface layers of the pool to its periphery, thus leading to a one and a half times increase in the penetration width compared to the calculation variant that ignored the melt convection. Figure 2 shows comparison of the calculation results on contours of the pool and heat-affected zone (see Table 1, No.4) with the experimental data, where the calculated shape of the penetration zone (curve *1*, isothermal line $T = 1480$ °C) and boundary of the heat-affected zone (curve *2*, isothermal line $T = 750$ °C) are superimposed on the macrosection.

As follows from Figure 2, the best agreement between the calculation and experimental data is observed with the simultaneous allowance for the thermal buoyancy and thermocapillary forces. It is likely that the difference between the calculation and experimental data on the shape of the molten zone is associated with deformation of the free surface of the pool under the effect of the vapour recoil reaction. Figures 3 and 4 show the field of isothermal lines on the plate surface and in a longitudinal section of the weld (coordinate $x = 0$ corresponds to the centre of the heat source).

It follows from Figures 3 and 4 that the maximal base metal penetration depth and width are

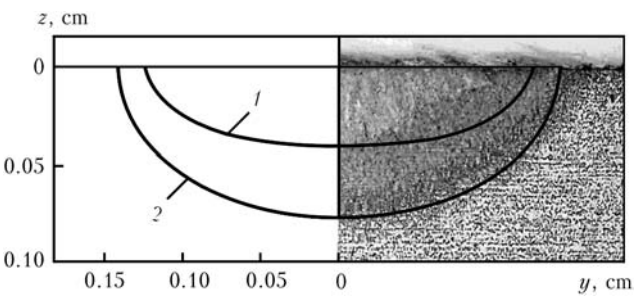

Figure 2. Penetration zone and heat-affected zone in laser heating (*1*, *2* — see the text)

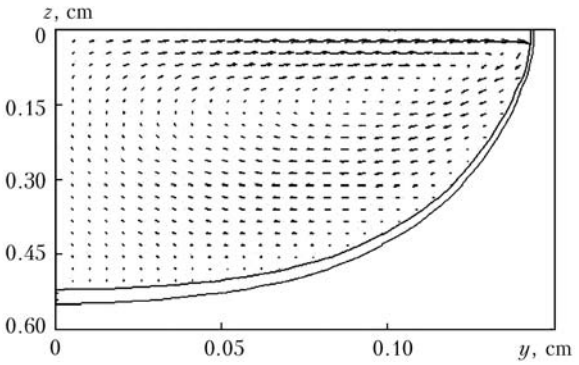

Figure 1. Field of the melt velocities in cross section of the metal pool (Table 1, variant No.4)

shifted from the source centre towards the tailing part to a distance of 0.06–0.08 cm.

Figure 5 shows thermal cycles at different sections in height of the plate. It follows from this Figure that the plate is heated to a temperature above 750 °C and to a depth of less than 0.3 cm at an average time of dwelling in the 800–500 °C range equal to 0.15 s.

Results of investigations of the effect of laser heating parameters (thermal power of laser radiation, heat spot radius, and heat source speed) are given in Tables 2–4.

Increase in power from 200 to 400 W leads to a 2.5 times increase in the penetration depth. Further increase in power ($P_L > 400$ W) does not exert a considerable effect on the penetration depth, as the maximal temperature of the surface of the molten metal pool becomes higher than the boiling temperature of the base metal of the plate, heat losses for evaporation of metal from the melt surface growing accordingly.

Consider peculiarities of heating of the plate under the effect of the combined laser-microplasma energy source. It was assumed in conducting the calculation experiment that centres of the laser and plasma heating spots coincided. The distribution of the power density of each of the

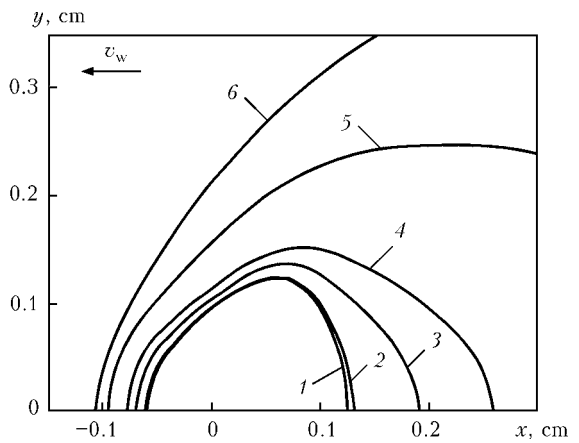

Figure 3. Field of isothermal lines on the plate surface at $T = 1480$ (*1*), 1430 (*2*), 1000 (*3*), 600 (*4*), 250 (*5*) and 100 (*6*) °C

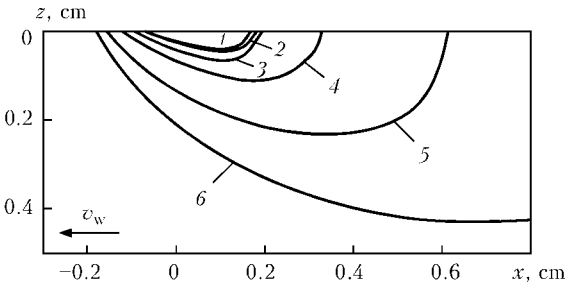

Figure 4. Field of isothermal lines in axial section of the weld at T = 1480 (*1*), 1430 (*2*), 1000 (*3*), 600 (*4*), 250 (*5*) and 100 (*6*) °C

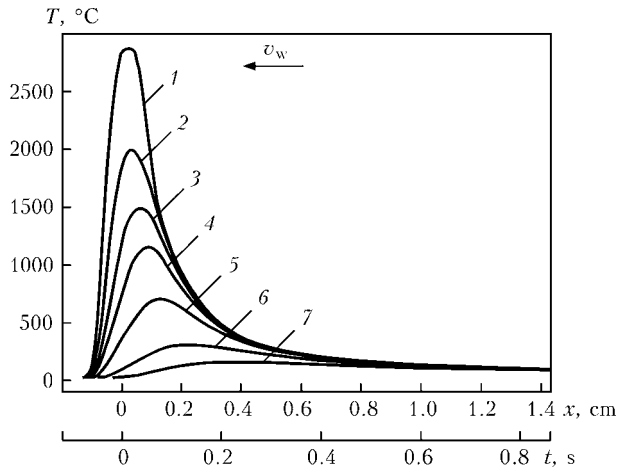

Figure 5. Temperature cycles at the weld axis for different sections in height of the plate at z = 0 (*1*), 0.02 (*2*), 0.04 (*3*), 0.06 (*4*), 0.28 (*5*), 0.36 (*6*) and 0.44 (*7*) cm

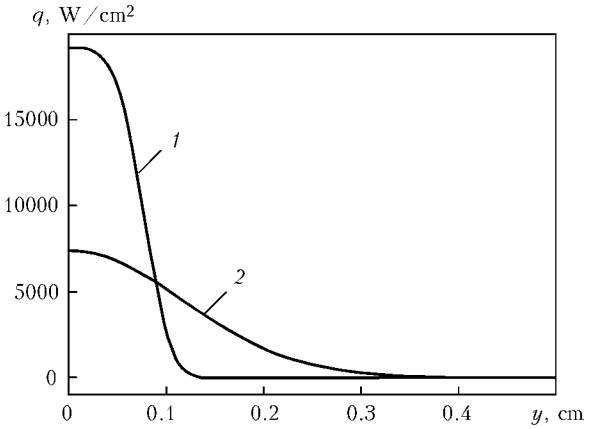

Figure 6. Distribution of specific heat flows of the laser (*1*) and plasma (*2*) heat sources on the plate surface (r_L = = 0.1 cm, efficiency = 0.32, P_L = 1250 W, r_P = 0.25 cm, efficiency = 0.5, P_P = 1300 W)

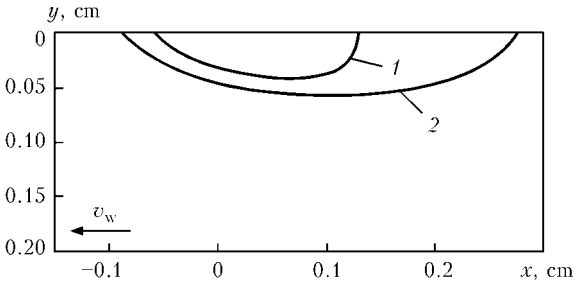

Figure 7. Shape of the penetration zone in axial section of the weld (T = 1480 °C) under the effect of the laser (*1*) and combined laser-microplasma (*2*) heat sources

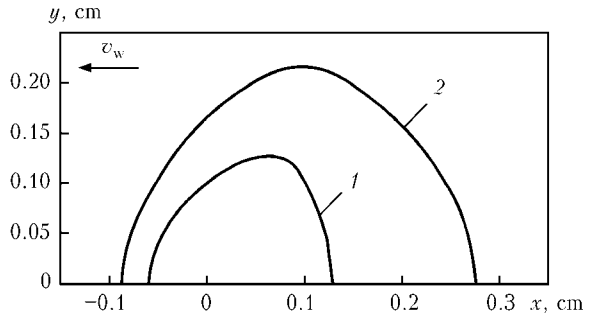

Figure 8. Shape of the penetration zone on the plate surface under the effect of the laser (*1*) and combined laser-microplasma (*2*) heat sources

said heat sources on the surface of the material treated is shown in Figure 6, where P_P is the plasma source power.

Figures 7 and 8 show the shapes of the penetration zones of the base metal in a longitudinal section and on the surface of the plate treated, respectively.

As indicated by the calculation data, under the effect of combined laser-microplasma heating

Table 2. Effect of the thermal power introduced into the plate on penetration parameters at v_w = 1.67 cm/s and r_L = 0.1 cm

P_L, W	H, cm	B, cm	T_{max}, °C	V_x, cm/s	V_y, cm/s
200	0.0165	0.1094	1886	12.8	3.7
300	0.0339	0.1872	2518	38.2	12.6
400	0.0418	0.2526	2880	51.3	16.5
500	0.0455	0.2826	2920	54.9	17.3
600	0.0475	0.3022	2944	57.1	17.9

Table 3. Effect of the heat spot radius on penetration at P_L = = 400 W and v_w = 1.67 cm/s

r_L, cm	H, cm	B, cm	T_{max}, °C	V_x, cm/s	V_y, cm/s
0.10	0.0418	0.2526	2880.65	51.30	16.50
0.12	0.0396	0.2338	2589.32	39.24	12.74
0.14	0.0346	0.2150	2274.98	27.45	8.42
0.16	0.0276	0.1920	2002.03	17.19	4.85
0.18	0.0171	0.1550	1748.69	7.62	2.04
0.20	0.0042	0.0712	1512.43	0	0

Table 4. Effect of the heat source speed on penetration at P_L = = 400 W and r_L = 0.1 cm

v_w, cm/s	H, cm	B, cm	T_{max}, °C	V_x, cm/s	V_y, cm/s
1	0.051	0.3220	2890	51.6	16.7
2	0.039	0.2320	2872	50.4	16.2
3	0.032	0.1860	2742	45.2	14.5
5	0.023	0.1480	2453	30.7	10.7
10	0.010	0.1040	1956	9.8	2.0

the width of the penetration zone increases 1.5 times, compared to laser heating. Due to this, the combined laser-microplasma treatment can provide a substantially larger size of the deposited bead.

Conclusion

With the laser heat source affecting the plate surface an intensive (~50 cm/s) sub-surface flow of the melt forms in the molten zone. This flow is caused by the dominant action of the thermocapillary force, which is generated due to a high temperature gradient (~7000 °C/cm) on the free surface of the metal pool. The flow, which is directed from the axial part of the pool towards the melting front, intensifies the energy transfer from the overheated paraxial part of the pool to its peripheral region, and favours increase in width of the molten zone. The effect of convective stirring of the pool to the penetration depth is much lower because of the mostly sub-surface flow of the melt. Application of the combined laser-microplasma energy source for cladding using powder materials (including bulk materials) allows increasing width of the deposited bead compared to laser cladding, and raising the productivity of the cladding process.

1. Duley, U. (1986) *Laser processing and analysis of materials*. Moscow: Mir.
2. Arutyunyan, R.V., Baranov, V.Yu., Bolshov, L.A. et al. (1989) *Effect of laser radiation on materials*. Moscow: Nauka.
3. Vedenov, A.A., Gladush, G.G. (1985) *Physical processes in laser treatment of materials*. Moscow: Energoatomizdat.
4. Rykalin, N.N. (1951) *Calculation of thermal processes in welding*. Moscow: Mashgiz.
5. Knight, Ch.J. (1979) Theoretical modeling of rapid surface vaporization with back pressure. *AIAA J.*, 17(**5**), 519–523.
6. Demchenko, V.F., Krivtsun, I.V., Semyonov, I.L. et al. (2009) Mathematical modelling of the processes of heating and convective evaporation of metals under the effect of pulse laser radiation. In: *Proc. of 4th Int. Conf. on Beam Technologies and Laser Application* (Saint-Petersburg, 23–25 Sept. 2009). Saint-Petersburg: StPPU, 81–85.
7. Lyashko, I.I., Demchenko, V.F., Vakulenko, S.A. (1981) Variant of the method for splitting of equations of dynamics of the viscous incompressible fluid on the Lagrangian–Eulerian networks. *Doklady AN USSR*. Series A, 43–47.
8. Demchenko, V.F., Lesnoj, A.B. (2000) Lagrangian–Eulerian method of numerical solution of multidimensional problems of convective diffusion. *Doklady NAN Ukrainu*, **11**, 71–75.

Received 24.01.2013